Supporting information

Identification of complete prokaryotic proteasome machinery in the parasite

We have earlier identified and characterized *P. falciparum* homolog of ClpQ protease (PfClpQ); the PfClpQ is a threonine protease that is expressed in the late stages of the blood stage parasite cycle.[15] With our objective to characterize the full prokaryotic proteasome machinery in *P. falciparum*, we attempted to identify the ClpY homologue in *P. falciparum* genome which is a chaperone like AAA+ ATPase component of this machinery. A sequence search at the PlasmoDB database using ClpY protein sequences of *Haemophilus influenza* and *E. coli* identified an open reading frame (PFI0355c), that codes for a putative translation product of 922 amino acids, as the *P. falciparum* ClpY orthologue (PfClpY). The C-terminal half of PFI0355c (485aa-922aa) showed high sequence similarity with orthologs of ClpY in different prokaryotes as well as apicomplexan and kinetoplastid parasites. Proteins domain analysis of PFI0355c by Pfam showed that this region contains an AAA (ATPase family associated with various cellular activities) domain (E-value $7.0e^{-42}$) that harbor the characteristic walker A and walker B motifs (Figure 1A). Alignment of the C-terminal half of PfClpY with ClpY homologos in prokaryotes showed that most of the highly conserved residues of their AAA domain (labeled as N-domain) and the C-terminal domain are either identical or similar in PfClpY (Figure S1A). An intermediate domain (I-domain) of 78aa was also found to be inserted between the walker A and walker B motifs of the AAA domain of PfClpY as in case of other ClpY orthologs. The I-domain show low level of homology among the ClpY proteins of prokaryotes and apicomplexa with several insertions and deletions. A structure model of PfClpY was generated based upon crystal structure of ClpQ of

Haemophilus Influenzae (PDB 1IM2). The structure model show that the I-domain has coiled helices that protrudes out of the N-domain at the distal-end while the C-domain consists of four helixes is present at the base (Figure S1B). Homologs of PfClpY were also identified from *P. berghei* (PBANKA_080890), *P. chabaudi* (PCHAS_080870), *P. vivax* strain SaI-1 (PVX_098815) and *P. yoelii yoelii* strain 17XNL (PY01951) from the genome database. An alignment of the predicted proteins sequences of these genes showed that the PfClpY protein is highly conserved in the *Plasmodium* spp.

Expression and purification of recombinant PfClpQ, PfClpY and its fragments, and characterization of peptidase and ATPase activity

To characterize the PfClpY protein and to study its interaction with PfClpQ, a large fragment of PfClpY (Figure 1A) harboring the N-, I- and C-domain was cloned and expressed in *E. coli*. The recombinant PfClpY was expressed as ~ 52kDa protein mainly in the insoluble fractions of the *E. coli* cells. PfClpY was obtained from the inclusion bodies pellet, purified under denaturing conditions on a Ni^{2+}-NTA column and refolded by rapid dilution method followed by ion exchange chromatography. Purified PfClpY migrated as a single band (~ 52kDa) on coommassie stained SDS-PAGE (Figure S3C). A pyrophosphate release assay was carried out to assess the ATPase activity of the recombinant PfClpY. As shown in Figure S3E, recombinant PfClpY showed ATPase activity in a concentration dependent manner. To rule out that the activity due to any contamination from the *E. coli* cells, fractions were also collected in same way from cultures of *E. coli* harboring only the pET expression plasmid; these fractions were used as control in the ATPase assay and did not showed any ATPase activity.

We also expressed a C-terminal fragment of PfClpY with Trx-fusion tag and purified by affinity chromatography on a Ni^{2+}-NTA column, the recombinant PfClpY-C showed an apparent mobility of ~ 40kDa (Figure S3D). In addition, a similar PfClpY-C fragment with 12 residue truncation at its C-terminus (PfClpY-ΔC) was expressed as a Trx-fusion that showed apparent mobility of ~ 40kDa in the SDS-PAGE (Figure S3D).

The protease domain of PfClpQ was expressed and purified (Figure S3A) as described earlier.[15] The *in vitro* activity assay using fluorogenic peptide substrate showed that the PfClpQ harbours threonine protease activity (Figure S3B).

Yeast two hybrid assay for PfClpQ and PfClpY fragments. The gene fragment corresponding to mature region of PfClpQ protein (112–510 bp; 38–170 aa) was amplified from total cDNA of the parasite by PCR using primers 566A, 5' GG CCC ATG GAG ATA TTA TGT GT AGGAA AAT 3' and 567A, 5' GC GGTCC TTA CAA TGT TTC ACA AAT AAA ATT 3'. The amplified PCR product was digested with NcoI and *BamH*I and cloned into *Nco*I and *BamH*I sites of pGBKT7 vector (BD Biosciences) to give pGBK-PfClpQ construct.

A large fragment of PfClpY (1453-2769bp, 385-922aa) harboring N-, I- and complete C-domains, was amplified from total cDNA of the parasite by PCR using primers 569A, 5' GG CCC ATG GAG TTA TAT CCT CAT GAG ATT GTG G 3' and 570A, 5' GCC GGA TCC TTA TAT GAT ATA TTT TTT TAA GTC GTA TTG C 3'. The amplified PCR product was cloned into NcoI and BamHI sites of pGADT7 vector (BD Biosciences) to give pGAD-PfClpY construct. A similar PfClpY fragment with 12 residue deletion at the C-terminus (PfΔClpY; 1453-2730bp, 385-910aa) was amplified

using primers 569A, and 571A, 5' gCC ggA TCC TTA AAT AAA ACC TTC CAg Cg 3'. The amplified PCR product was also cloned into *Nco*I and *BamH*I sites of pGADT7 vector (BD Biosciences) to give pGAD-PfΔClpY construct.

In addition, a C-terminus fragment of PfClpY labeled as PfClpY-C (2176-2769bp; 725-922 aa), was amplified using primers 601-2A, and 570A. A similar C-terminus fragment with 12 residue deletion at the C-terminus labeled as PfClpY-ΔC (2176-2730bp; 725-910 aa) was amplified using primers 601-2A and 571A. The two fragments were also cloned in pGAD vector to give constructs pGAD-PfClpY-C and pGAD-PfClpY-ΔC respectively.

The pGBKT7-PfClpQ construct was co-transformed with each of the PfClpY construct into the AH109 yeast cells, and potential interacts were assessed by growth of the co-transformants on selective media.

Uptake and localization of biotin-labeled Ant-FI peptide in the parasite. To ascertain the uptake and localization of the Ant-FI peptide in the parasite, biotinylated-Ant-FI peptide was used. The trophozoite stage parasites were incubated with biotinylated-Ant-FI peptide at a final concentration of 50μM for 2h. The parasites were washed and stained with MitoTracker Red CMXRos (Invitrogen) (at a final concentration of 20 nM in 1× PBS) for 30 min at 37°C; subsequently the parasites were washed and fixed in paraformaldehyde - glutaraldehyde in 1×PBS and stained with FITC-streptavidin. These parasites were stained with DAPI at a final concentration of 2 μg/ml for 30 min at 37°C and viewed using a Nikon TE 2000-U fluorescence microscope (Figure S5).

Table S1: Amino acid sequences of different synthetic peptides used in the study.

Peptide	**Amino acid sequence**
FI	FIKQYDLKKYII
Dansyl-FI	Dansyl-FIKQYDLKKYII
Ant	RQIKIWFQNRRMKWKK
Ant-FI	RQIKIWFQNRRMKWKKFIKQYDLKKYII
Ant- Scrambled FI (Ant-Scr)	RQIKIWFQNRRMKWKKFLYKIKQDIKYI

Table S2: Growth of yeast AH109 cells on different selection meda (with amino acid dropout) after co-transformation with pGBK-PfClpQ plasmid construct and a pGAD construct harboring PfClpY fragment

Transformation constructs	**Selection media with drop-outs**			
	SD(Leu^-)	SD (Leu^- Try^-)	SD (Leu^- Try^- His^-)	SD (Leu^- Try^- His^-) + ATH (12mM)
pGBKT7 vector control	+++	-	-	-
pGADT7 vector control	-	-	-	-
pGBKT7 + pGADT7 vector control	+++	++	+	-
pGBK-PfClpQ + pGAD-PfClpY	+++	+++	++	++
pGBK-PfClpQ + pGAD-PfΔClpY	+++	+++	+	-
pGBK-PfClpQ + pGAD-PfClpY-C	+++	+++	++	++
pGBK-PfClpQ + pGAD-PfClpY-ΔC	+++	+++	+	-
Negative control constructs	+++	++	+	-

Supplementary Figure legends:

Figure S1: (A) Amino acid sequence alignment of *P. falicparum* ClpY (PfClpY) with that of ClpY homologs from other organisms; *Bacillus amyloliquefaciens*, *Listeria monocytogenes, Staphylococcus auerus*, *Escherichia coli*, *Haemophilus influenzae*. Amino acids that are identical in at least three of the all species (>50%) are shown in dark. Amino acids that are similar in at least three of the all species (>50%) are shown in grey. The N-domain regions are marked with blue line, the Walker-A and Walker-B domains are marked with boxes. The I-domain is marked with pink line and the C-domain is marked with green line. (B) 3D structure model of mature PfClpY; N, I and C-domains are marked.

Figure S2: Stage specific expression of PfClpQ and PfClpY in asexual blood stage parasites. Relative transcription of *pfclpQ* and *pfclpQ* assessed by real-time-RT-PCR using total RNA extracted from tightly synchronized parasite cultures at early ring (ER), late ring (LR), trophozoite (T), late trophozoite (LT), early schizont (ES) and late schizont (LS) stages (8, 16, 24, 32, 40 and 48 h after invasion). Stage specific expression of *eba-175* and *falcipain 2* were also analyzed as controls. The 18S rRNA amplification was used as normalization control to calculate the relative transcription of these genes for each sample.

Figure S3: Expression, purification and characterization of recombinant PfClpQ protease and PfClpY ATPase. (A) SDS-PAGE showing purified recombinant protein

corresponding to the mature protease domain of PfClpQ. (B) Protease activity assay of recombinant PfClpQ using fluorometric assay: the recombinant PfClpQ protein was allowed to cleave an AMC linked fluorogenic peptide substrate (Suc-GGL-AMC; 50μM) and release of the free AMC at different time points was measured using a fluorometer. (C) SDS-PAGE showing purified recombinant protein harbouring the N-I-C domains of PfClpY. (D) SDS-PAGE showing purified recombinant protein corresponding to the C-domain of PfClpY (PfClpY-C, lane 1) and its truncated version (PfClpY-ΔC, lane 2). (E) ATPase activity of recombinant PfClpY: thin layer chromatography showing pyrophosphate (^{32}P) release assay using different concentration (1, 2 and 3μg) of recombinant PfClpY (lane 1-3) and γ^{32}P-ATP. Control reactions were carried out with buffer alone (lane 4).

Figure S4: Yeast two hybrid analysis showing interaction of PfClpQ with PfClpY and its C-terminal fragment (PfClpY-C) and their truncated constructs (PfΔClpY and PfClpY-ΔC respectively). The pGBK-PfClpQ construct was co-transformed with each of the PfClpY construct into the AH109 yeast cells, and potential interactions were assessed by growth of the co-transformants on selective media.

Figure S5: Fluorescent microscopic images showing uptake and localization of biotin-labeled Ant-FI peptide in the parasite. Parasites were incubated with 50μM of biotin-labeled Ant-FI peptide for 2h, mitochondria were stained with Mitotracker (red), fixed and stained with FITC labeled streptavidin. Parasite nuclei were stained with DAPI (blue) and parasites were visualized by fluorescence microscope.

Figure S6: Reversal of growth inhibition by removal FI-peptide in the culture. Tightly synchronized early trophozoite stage parasite cultures (~30h post-invasion) were treated with Ant-FI peptide at 50μM (~EC_{50}); the parasite samples were washed at different time point and then allowed to grow for 24h for formation of new ring, percentage parasite growth inhibition was estimated as compared to unwashed culture.

Figure S7: In situ estimation of mitochondrial membrane potential of *P. falciparum* parasite by JC-1 staining after treatment with Ant-FI peptide. Flow cytometry dot blots of JC-1 green (FL-1) and JC-1 red (FL-2) of parasite population from cultures treated with Ant-FI (90μM) or solvent alone for 3h. The parasite population with high and low JC1 aggregate (red) staining are marked as R1 and R2 respectively. The Ant-FI treated parasite culture show reduction in cell population with JC-1 red staining.

Figure S8: Activation of CaspACE-VAD-FMK binding cystein proteases in *P. falciparum* parasite. Flow cytometry dot blots for parasite population showing CaspACE tagged parasites in the cultures at different time points (4, 6, 8, and 16h) after treatment with peptides Ant-FI (90μM), Ant-Scrambled (Ant-Scr; 90μM) or solvent alone. Percentage of CaspACE tagged parasite (quadrant R2) is also shown. At 8h and 16h after treatment there was some decrease in the total parasite population due to parasite death.

Figure S9: Fluorescent microscopic images showing labeling of CaspACE-VAD-FMK in *P. falciparum* parasite after treatment with peptides Ant-FI (90μM).

A

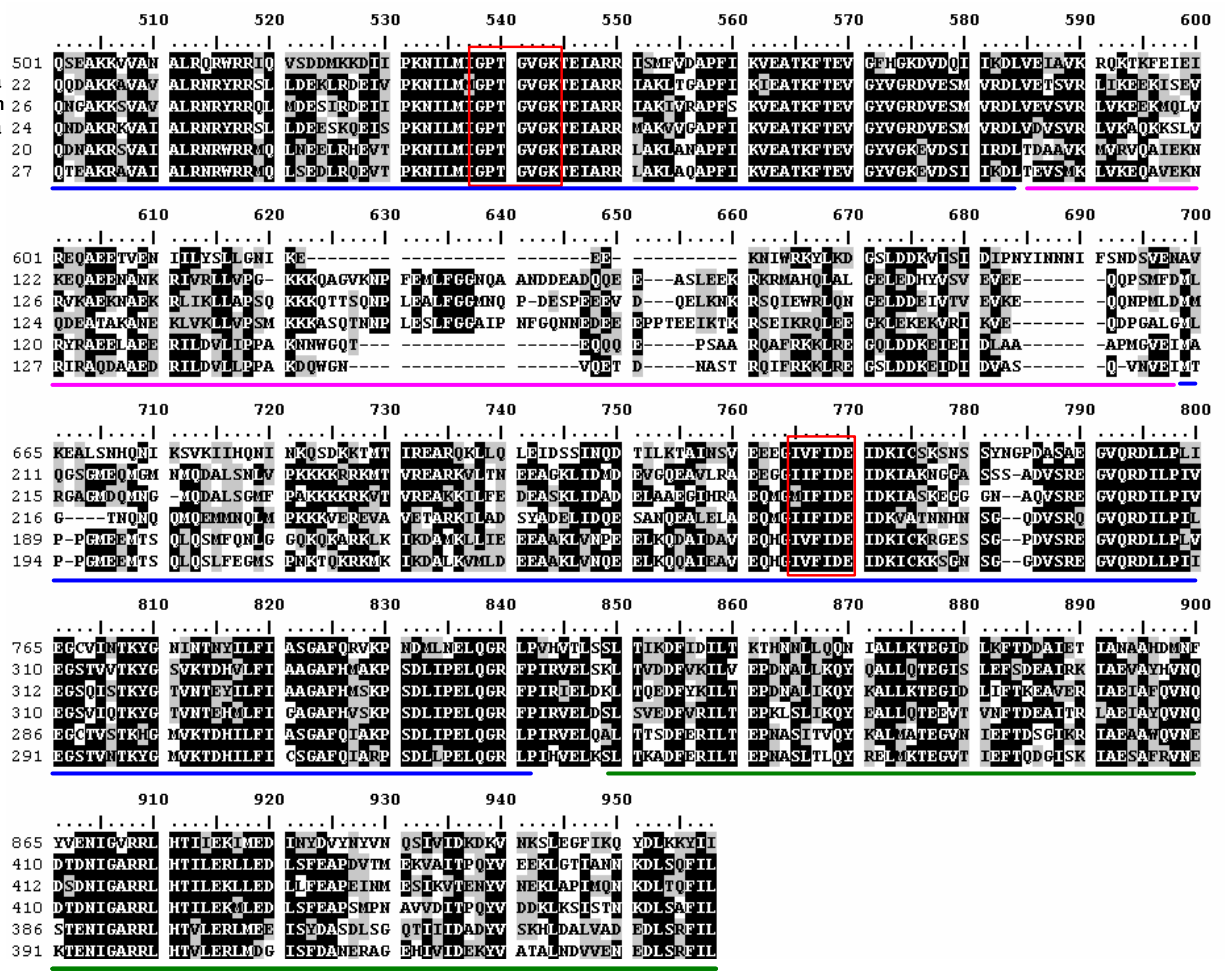

B

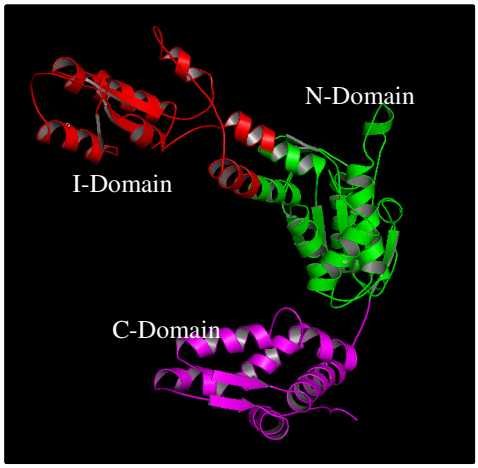

Figure S1

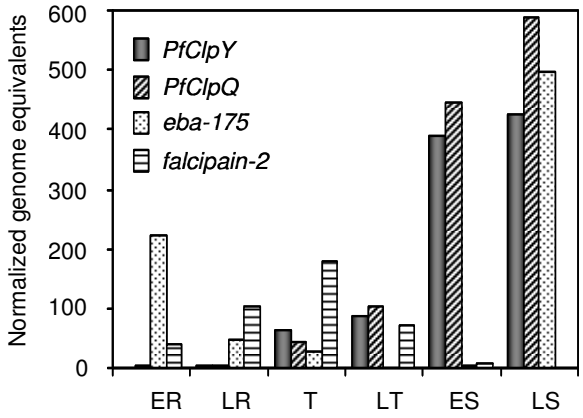
Normalized genome equivalents
600
500
400
300
200
100
0
PfClpY
PfClpQ
eba-175
falcipain-2
ER
LR
T
LT
ES
LS

Figure S2

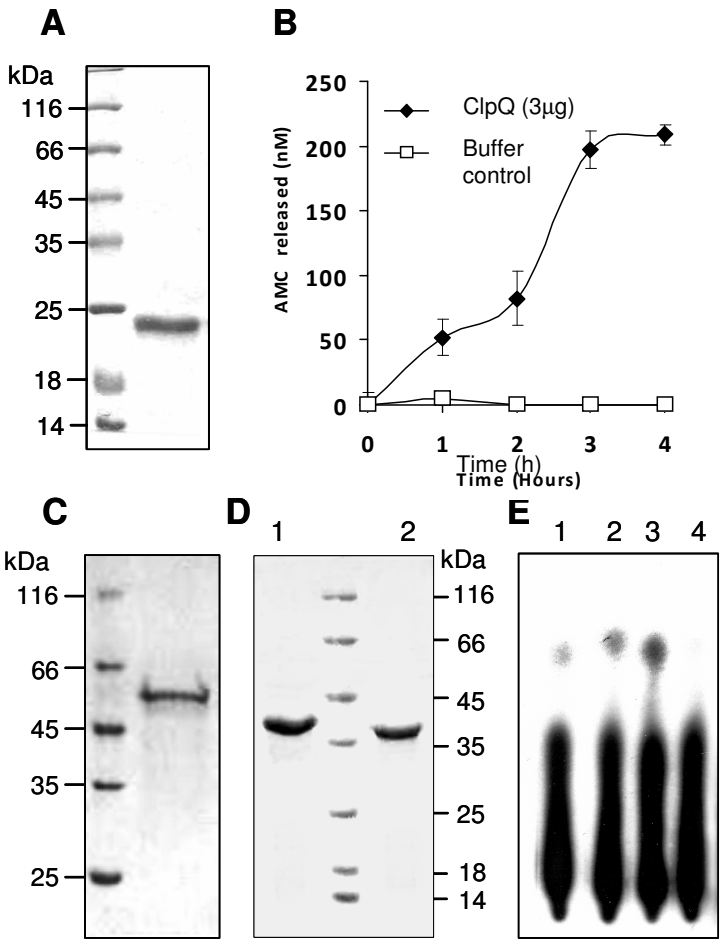
A
kDa
116
66
45
35
25
18
14
B
250
200
150
100
50
0
AMC released (nM)
ClpQ (3µg)
Buffer control
0
1
2
3
4
Time (h)
Time (Hours)
C
kDa
116
66
45
35
25
D
1
2
kDa
116
66
45
35
25
18
14
E
1
2
3
4

Figure S3

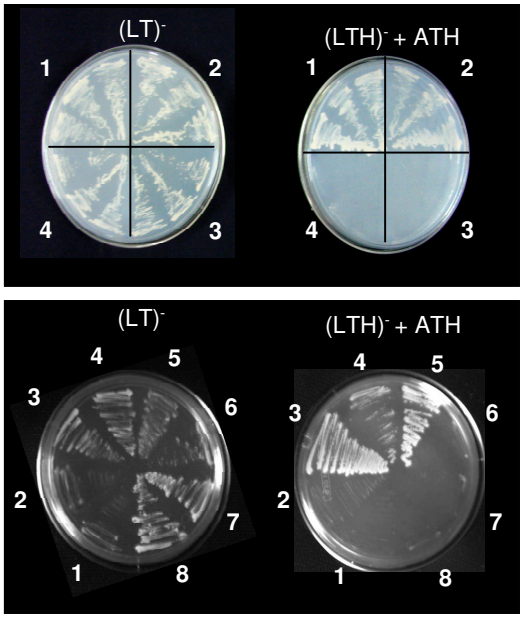

1. Positive control constructs
2. pGBKT7-PfClpQ + pGAD-PfClpY
3. pGBKT7-PfClpQ + pGAD-PfΔClpY
4. Negative control constructs

1. pGBKT7 vector control
2. pGAD vector control
3. Positive control
4. pGBKT7-PfClpQ + pGAD-PfClpY-ΔC
5. pGBKT7-PfClpQ + pGAD-PfClpY-C
6. Negative control constructs
7. Negative control constructs
8. pGBKT7 + pGAD vector control

Figure S4

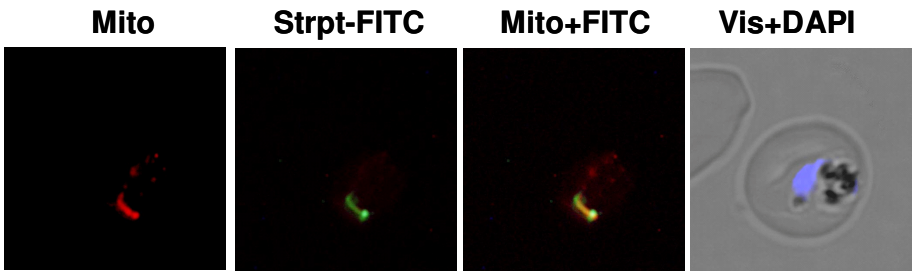

Figure S5

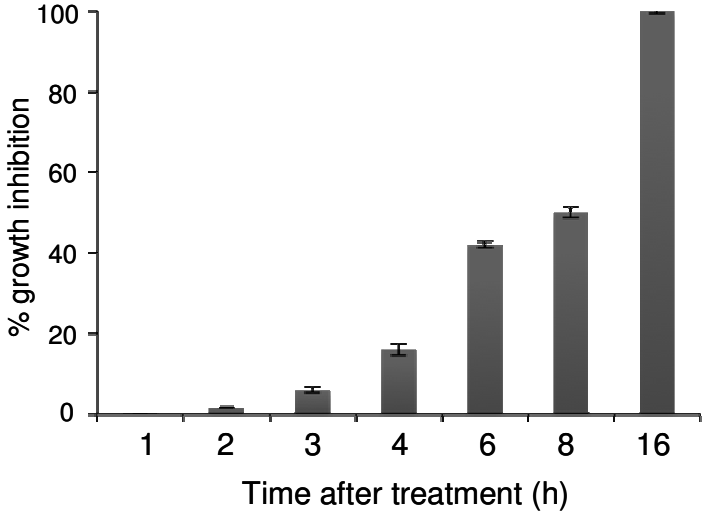
100
80
60
40
20
0
% growth inhibition
1
2
3
4
6
8
16
Time after treatment (h)

Figure S6

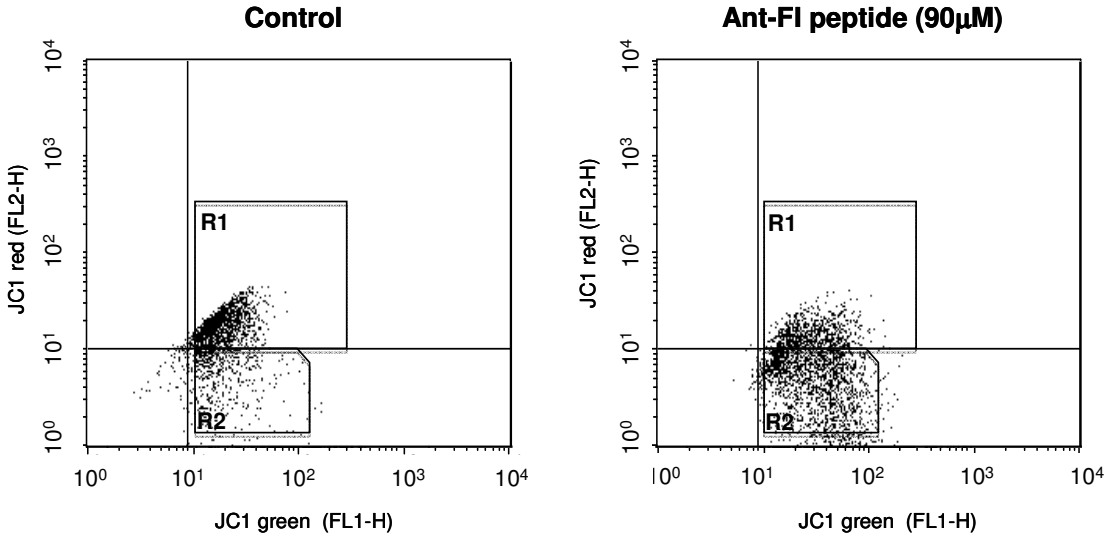
Control
Ant-FI peptide (90μM)
JC1 red (FL2-H)
JC1 green (FL1-H)
R1
R2
10^0
10^1
10^2
10^3
10^4

Figure S7

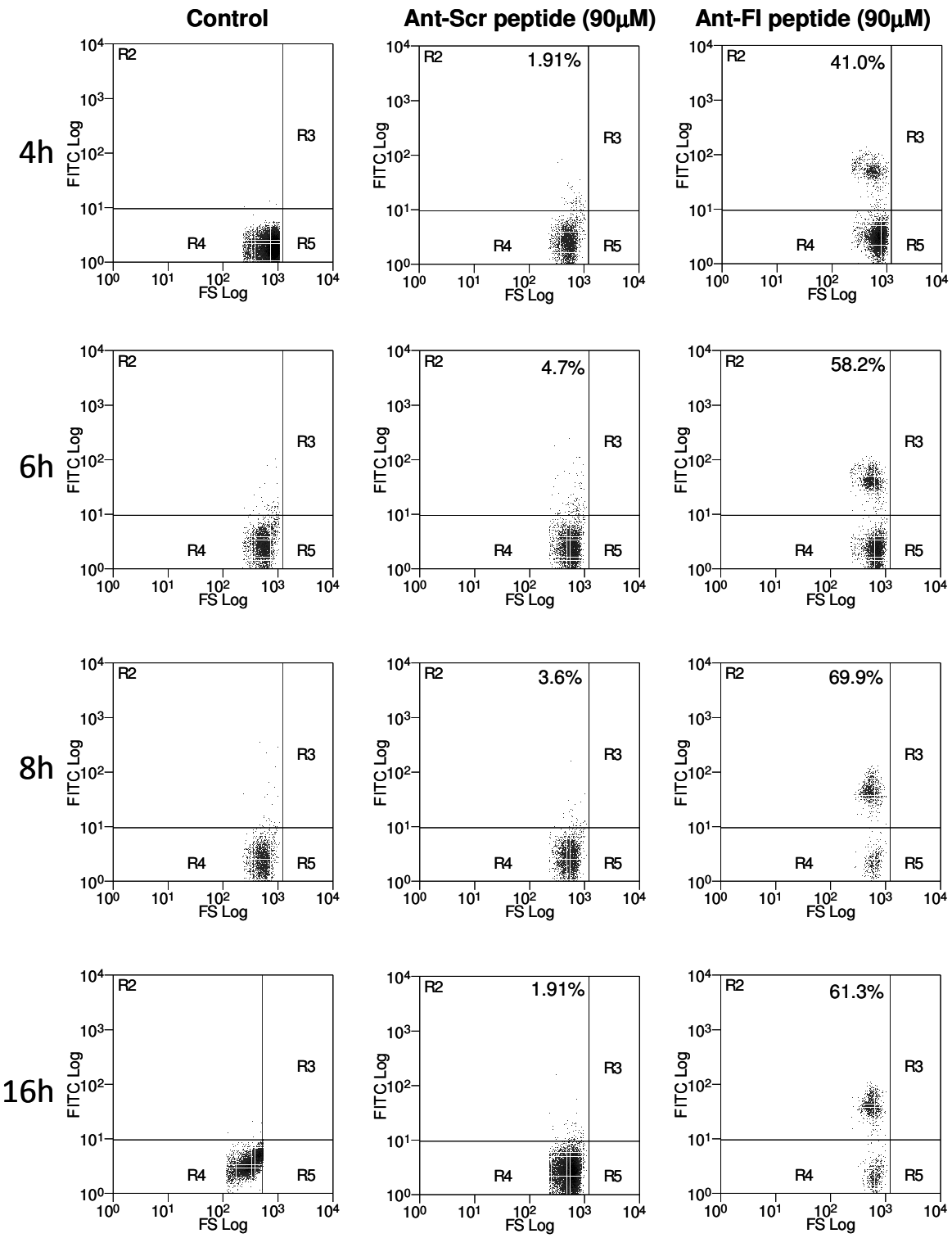
Control
Ant-Scr peptide (90μM)
Ant-Fl peptide (90μM)
4h
6h
8h
16h
R2
R3
R4
R5
1.91%
41.0%
4.7%
58.2%
3.6%
69.9%
1.91%
61.3%
FITC Log
FS Log

Figure S8

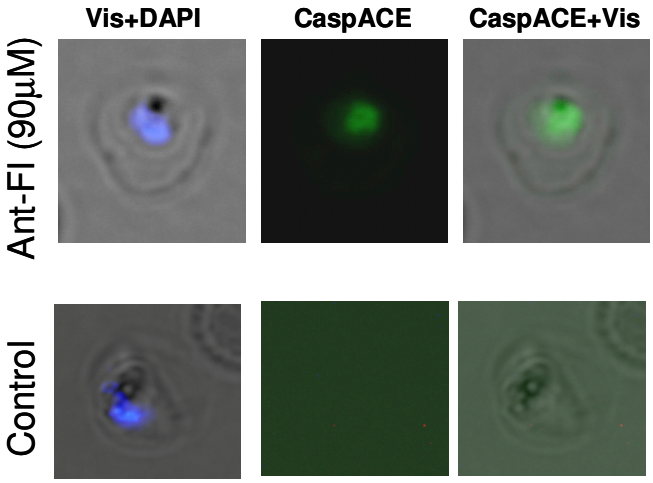

Figure S9